The 2009 IEEE/RSJ International Conference on
Intelligent Robots and Systems
October 11-15, 2009 St. Louis, USA

Detection of Non-flat Ground Surfaces Using V-Disparity Images

Jun Zhao, Mark Whitty and Jayantha Katupitiya
ARC Centre of Excellence for Autonomous Systems
School of Mechanical and Manufacturing Engineering
The University of New South Wales, Sydney, NSW 2052, Australia
J.Katupitiya@unsw.edu.au

***Abstract*— Ground plane detection plays an important role in stereo vision based obstacle detection methods. Recently, V-Disparity image has been widely used for ground plane detection. The existing approach based on V-Disparity image can detect flat ground successfully but have difficulty in detecting non-flat ground. In this paper, we discuss the representation of non-flat ground in V-Disparity image, based on which we propose a method to detect non-flat ground using V-Disparity image.**

***Index Terms*— V-disparity image, correlation, stereo vision.**

I. Introduction

Stereo vision is one of the key components in vision-based robot navigation. Detecting the surrounding environment of a moving vehicle is a complex and challenging task. One of the key task of stereo vision is to detect the set of obstacles in the environment, which can be other vehicles, objects on the side of the robot's path, pedestrians, etc. The output of stereo vision is a depth map, in which the pixel information represents not the color, but the depth information of the field of view. Active sensors, such as laser or radar, can provide some kind of 3D information of the surrounding area, they also present some intrinsic limitations to their functioning, as mentioned in [1].

Because a vision system provides a large amount of data, extracting refined information sometimes may be complex. In obstacle detection tasks, the purpose is to distinguish the obstacle pixels from the ground pixels in the depth map. Se and Brady [2] quote from Gibson's "ground theory hypothesis"(1950): "there is literally no such thing as a perception of space without the perception of a continuous background surface". In this study, we assume that the ground can be locally represented by a plane [3].

"Plane fitting" is a traditional method for ground estimation and used by different researchers. In [4] , the authors used *RANSAC Plane Fitting* to find the disparity of ground pixels. In [5], pixels (u, v) with a valid value in the depth map are labeled as belonging to the ground plane if the following constraint is satisfied: $d(u, v) \leq au+bv+c+r(d)$ where (a, b, c) are the ground plane image parameters and $r(d)$ is a relaxation on the planar constraint. In [6], the authors developed a road detection algorithm utilizing road features called plane fitting errors.

In recent years, V-Disparity image has been widely used for ground plane estimation [1][7][8][9]. In V-Disparity image, the abscissa (w) plots the offset for which the correlation has been computed; the ordinates (v) plots the image row number; the intensity value is settled proportional to the measured correlation, or the number of pixels having the corresponding disparity (w) in a certain row (v). Each planar surface in the field of view is mapped in a segment in the V-disparity image [8]. Vertical surfaces in the 3D world are mapped into vertical line segments, while ground plane in the 3D world are mapped into slanted line segment. This line segment, called ground correlation line in this study, contains the information about the cameras pitch angle at the time of acquisition (mixed with the terrain slope information).

Both plane fitting and V-Disparity image are based on flat ground assumption. This is a poor model since deviation from the flat ground or may be as large as or larger than the obstacles we wish to detect. In consequence the road object separation and the 3D objects position estimation can be wrong. Therefore a non-flat ground assumption is compulsory for a robust obstacle detection methods. In [8], the authors used Hough Transform to extract the piecewise linear curve in V-Disparity image. In this paper, we discuss the representation of the non-flat ground in the V-Disparity image and introduce a method to extract this non-flat ground correlation line in V-Disparity image not using Hough Transform. In Section II, we first explain the principle of V-Disparity image, and an important property of it. In Section III, we discuss the representation of ground correlation line in V-Disparity image, then introduce a method to extract this line in Section IV. In Section V, we show some experimental results. In Section VI, we draw our conclusion.

II. V-Disparity Image and its property

To obtain a real world representation from an image pair, it is necessary to know the cameras placement at the time of acquisition. Consider cameras on an autonomous vehicle that are tilted down an angle θ, as shown in Fig. 1. In this figure, a camera centered coordinate system, xyz, defines the positions of points in the physical world in front of the cameras. If the cameras are a distance h above the ground, the ground plane can be represented as

$$z = \frac{h}{\sin\theta} - y\frac{\cos\theta}{\sin\theta} \tag{1}$$

An image coordinate system, uvw, defines the spatial positions of data points on the image plane (uv) and the relative

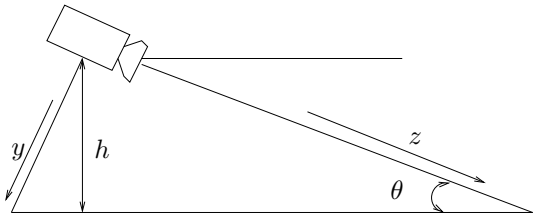

Fig. 1. Camera placement.

disparity of corresponding points between the left and right images (w). We adopt the pin-hole camera model, then the relationship between the world coordinates of a point $P(x, y, z)$ and the coordinates on the image plane (u, v) in the camera is

$$u = x\frac{f}{z}, v = y\frac{f}{z}, w = b\frac{f}{z} \tag{2}$$

where f is the focal distance of the lens and the stereo baseline is b.

From Eq. 1 and Eq. 2, we can get that in image plane

$$v = \frac{hw}{b\cos\theta} - f\tan\theta \tag{3}$$

In this equation, b and f are constants dependent on the camera geometry and spacing between cameras. In this study, we also assume that the camera height h is also fixed, that is, there only exists pitch variation. Thus v is a function of w and θ. At the time of acquisition, θ is also fixed, then the slope g of ground plane in V-Disparity image, can be represented as

$$g = \frac{\partial v}{\partial w} = \frac{h}{b\cos\theta} \tag{4}$$

One important property of ground correlation line in V-Disparity image is that, the behavior of the ground correlation line during a pitch variation is to oscillate, parallel to itself as shown in Fig. 2. Claudio et al [1] have experimentally found out this property. In [10], we investigate this characteristic mathematically and give the condition for this characteristic to be valid, which is, for a given $\triangle w$ and certain pitch oscillation, we need to reduce θ. Originally, labayrade [8] used Hough Transform to extract the ground correlation line from the V-Disparity image. Given this property, the slope and position of the ground correlation line in stable conditions can be achieved off-line during calibration stage. then under driving conditions the ground correlation line must be one of those parallel to the ground correlation line in stable condition and within a certain disparity range as shown in Fig. 2.

III. NON-FLAT GROUND GEOMETRY

Solid line in Fig. 3 shows the profile of the ground plane having two gradients, in this situation, the ground correlation line in V-Disparity image would be two straight lines as shown in Fig. 4

Dashed line in Fig. 3 shows the profile of the ground plane of which the gradient is changing gradually. In this situation,

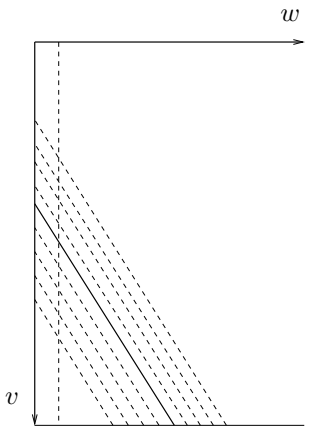

Fig. 2. Ground correlation lines in V-Disparity image. The solid slanted line corresponds to the ground correlation line obtained using the static calibration data, while the dashed slanted lines are the ones expected varying the pitch value. The solid vertical axis represents the 0 disparity value, the dashed vertical line indicates the disparity value of points at infinite distance; they do not overlap due to a slight convergence of cameras optical axes.

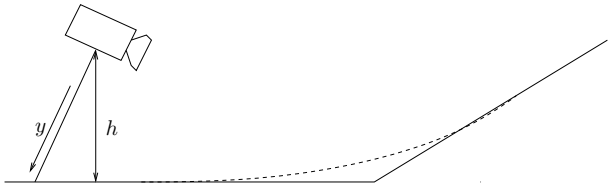

Fig. 3. Road profile. Sold line represents planar ground, dashed line represents curved ground

we adapt the expression of road curvature as in [11][12]:

$$y = \frac{h}{\cos\theta} - z\frac{\sin\theta}{\cos\theta} + C_{0,v}z^2 \tag{5}$$

where:

- θ is the pitch angle of the car
- $C_{0,v}$– road curvature in a vertical plane

From Eq. 5 and 2, we can get that in image plane,

$$v = \frac{hw}{b\cos\theta} - f\tan\theta + C_{0,v}\frac{bf^2}{w} \tag{6}$$

the slope g of ground plane in V-Disparity image, can be represented as

$$g = \frac{\partial v}{\partial w} = \frac{h}{b\cos\theta} - C_{0,v}bf^2w^{-2} \tag{7}$$

Eq. 7 shows that the slope g is also changing gradually, and it becomes greater when w becomes smaller. The rate of change of g with respect to w is,

$$l = \frac{dg}{dw} = C_{0,v}bf^2w^{-3} \tag{8}$$

thus the absolute value of l becomes greater when w becomes smaller. Suppose the gradient of ground plane under the vehicle is $g_s = (h/b)\sec\theta_s = \triangle v/\triangle w$ as shown in Fig. 5. In V-Disparity image the resolution of abscissa (w) is one pixel. If $\triangle v$ is fixed, from this figure we can see that the next distinguishable gradient bigger than g_s is

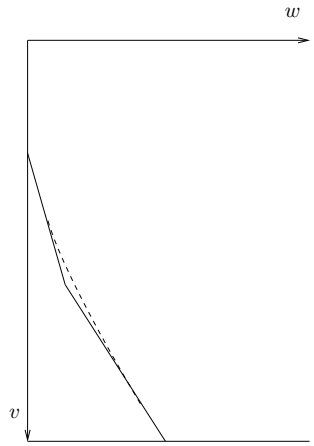

Fig. 4. V-Disparity image. Sold line represents planar ground, dashed line represents curved ground.

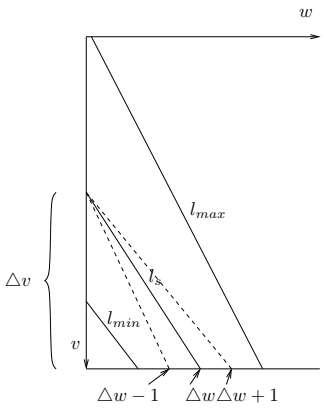

Fig. 5. Slope of ground correlation line during pitch variation. The solid slanted lines represent ground correlation lines. The dashed slanted lines represent the next distinguishable larger(associated with $\triangle w - 1$) and smaller(associated with $\triangle w + 1$) slopes near l_s.

$\triangle v/(\triangle w - 1)$. From Eq. 8 we can see that the slope g is changing slowly when w is large, that is, in the area nearest to the vehicle. Thus we can assume that the ground in the vicinity of the vehicle is flat. This assumption is widely used, in [12] the authors assume that the effect of the curvature can be sensed only after a 30m interval in their configuration.

Suppose the gradient of the ground near the vehicle is g_1, the gradient of the ground furthest from the vehicle is g_2. Because the ground in the vicinity of the vehicle is flat, the slope changing occurs when w is small. Also from Eq. 8 we can see that the slope g is changing rapidly when w is small, thus we can assume that the change of disparity $\triangle w$ corresponding to the change of slope $g_2 - g_1$ is small. Then we can approximate the ground correlation line in V-Disparity image to two straight line segments as shown in Fig. 4.

Consider the situation in Fig. 6, in this V-Disparity image the lower slanted line has gradient g_1, the upper g_2. Because the resolution of disparity is one pixel, the resolution of gradient g_1 is bounded by the two lower thick slanted lines as shown in the figure. Similarly, the resolution of gradient g_2 is bounded by the two upper thick slanted lines. These

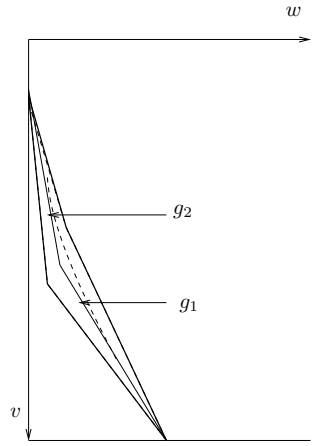

Fig. 6. Boundary of gradient g_1 and g_2.

Fig. 7. Example of a non-flat ground V-Disparity image.

four thick line segments form a close area. Any curved lines in this area could be seen as the combination of the straight lines having gradient g_1 and g_2. The dashed line is one such curved line.

Through observation of a lot of non-flat ground V-Disparity images, we found that the ground correlation line can be seen as the combination of two straight lines. One such example can be seen in Fig. 7. In [8], the authors used Hough Transform to extract the ground correlation line, however, it relied heavily on distinct road features which may not exist. In this paper, based on the fact that the ground correlation line can be seen as the combination of two straight lines, we introduce a method to extract this curve without using Hough Transform. Indeed, in the vicinity of the vehicle, or in other words, in the lower part of the image, the road is planar. Earlier in the paper, we have said that the behavior of the ground correlation line during a pitch variation is to oscillate, parallel to itself. Thus we can first find the ground correlation line in the vicinity of the vehicle by choosing from these parallel lines the one that has the highest accumulated grey level. Then, the problem is focused on how to find the ground correlation line furthest from the vehicle, that is, where it will depart from the ground correlation line in the lower part and its gradient.

IV. Ground Line Detection for Non-flat Ground

Suppose the gradient of ground correlation line close to the vehicle is g_0 as shown in Fig. 8(a), then the next

distinguishable gradient bigger than g_0 is g_1, and $g_1 = \Delta v/(\Delta w - 1)$. Accordingly, $g_m = \Delta v/(\Delta w - m)$, m is bounded by the greatest possible positive gradient of the ground. Similarly, the next distinguishable gradient smaller than g_0 is g_{-1}, and $g_{-1} = \Delta v/(\Delta w + 1)$. Accordingly, $g_{-n} = \Delta v/(\Delta w + n)$, n is bounded by the smallest possible negative gradient of the ground.

In the V-Disparity image, part of the ground correlation line in which $w > w_0$ is straight because the ground in the area closest to the vehicle can be considered as a plane, then the slope changing occurs in the disparity w in which $w < w_0$.

According to these, the process of finding the curved ground correlation line is as shown in Fig. 8. The slope and position of the ground correlation line close to the vehicle in stable condition can be achieved off-line during calibration stage. Then under driving conditions the ground correlation line must be one of those parallel to the ground correlation line in stable condition and within a certain disparity range as shown in Fig. 8(a). Then we can accumulate the corresponding measured correlation along each candidate line and choose the one has the highest value as shown in Fig. 8(b). Based on this ground correlation line close to vehicle, the possible slope changing are shown in Fig. 8(c). If the ground is non-flat, according to the discussion in last section, the ground correlation line can be approximated by a combination of two straight line segments. The lower line segment is the lower part of the slanted solid line having gradient g_0, the upper line segment is one of the dashed lines, it departs from the lower line segments at a disparity $w \leq w_0$, and has a gradient greater or smaller than g_0. The dashed lines in Fig. 8(c), together with the slanted solid line, show all the possibilities of the road curvature. We choose between these curvatures as follows: for each pixel on the curve, the corresponding measured correlation is accumulated. The curve is chosen with respect to the best score obtained as shown in Fig. 8(d).

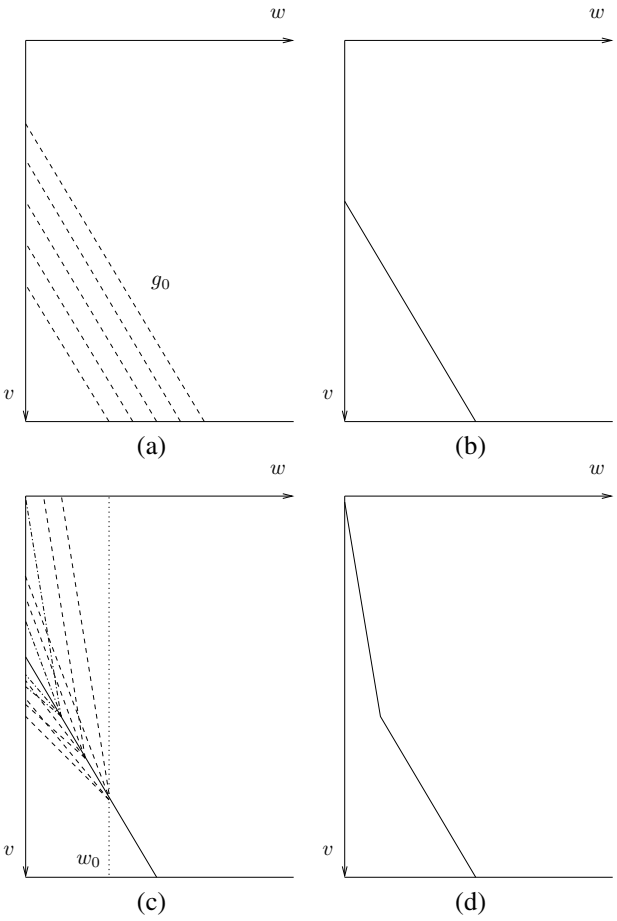

Fig. 8. Process of finding non-flat ground correlation line.

Fig. 9. Off road image with non-flat ground and disparity image.

V. Experimental results

We tested the method on images with non-flat ground. The disparity maps were computed using normal correlation based algorithms.

Fig. 9 shows an image with non-flat ground and the corresponding disparity image. Fig. 10(a) shows the V-Disparity image of Fig. 9. If the ground is considered flat, the ground correlation line would be that shown as red slanted line in this figure. Fig. 10(b) also shows the detected obstacles represented as red pixels. We can see that in this situation some ground pixels are seen as obstacles.

Fig. 11 shows the plot described in Fig. 8(c). The x axis(Disparity) shows the searched disparity range, the y axis(Gradient) shows the gradient range for each disparity, the z axis(Measured correlation) shows the corresponding measured correlation. From this plot we can see the maximum is unique. This maximum corresponds to the gradient changing disparity, and the gradient of the upper ground correlation line segment.

Fig. 12 shows the detected ground correlation line if the ground is considered non-flat, which has two straight lines. The detected gradient changing level is also shown as the red horizontal line in figure. Based on this non-flat ground correlation line, the detected obstacles are shown as red pixels in this Fig. 12(b). We can see that the false obstacle pixels appearing in Fig. 10 have been eliminated.

An image with a roadway is shown in Fig. 13. If the ground is considered flat, the ground correlation line and the detected obstacles would be shown in Fig. 14. We can see that some ground pixels are considered as obstacles. Fig. 15 shows the corresponding plot. Fig. 16 shows the detected ground correlation line if the ground is considered non-flat, and the corresponding detected obstacles.

Another image with a side walk is shown in Fig. 17, if the ground is considered flat, the ground correlation line

(a) (b)

Fig. 10. V-Disparity image and detected obstacles if ground is considered flat for image in Fig. 9.

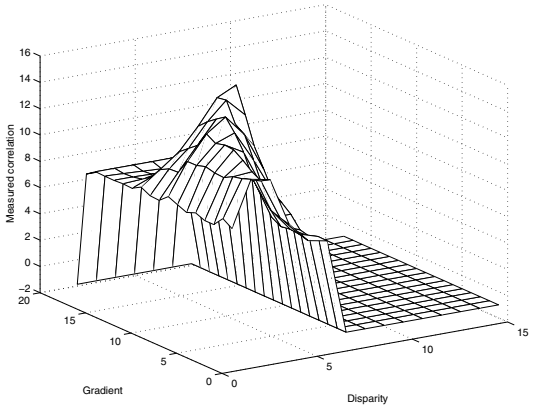

Fig. 11. Measured correlation plot for image in Fig. 9.

(a) (b)

Fig. 12. V-Disparity image and detected obstacles if ground is considered non-flat for image in Fig. 9.

Fig. 13. On road image with non-flat ground and disparity image.

(a) (b)

Fig. 14. V-Disparity image and detected obstacles if ground is considered flat for image in Fig. 13.

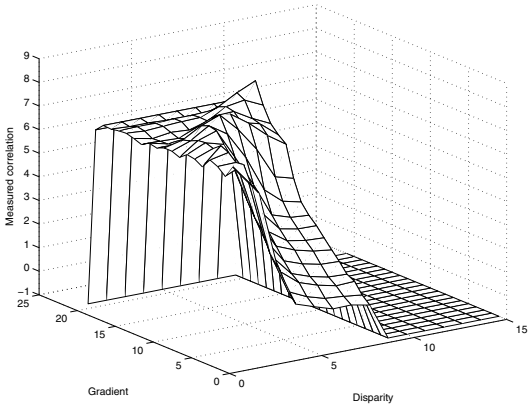

Fig. 15. Measured correlation plot for image in Fig. 13.

and detected obstacles would be as that shown in Fig. 18, we can see that some ground pixels are considered as obstacles. Fig. 19 shows the corresponding plot. Fig. 20(a) shows the detected ground correlation line, and Fig. 20(b) the detected obstacles if the ground is considered non-flat.

On a normal computer system(P4 2.8GHz processor and 1GB RAM), the computational time is less than 50ms, as the measured correlation needed in this algorithm have been calculated in the stereo matching stage, which is prior to obstacle detection.

(a) (b)

Fig. 16. V-Disparity image and detected obstacles if ground is considered flat for image in Fig. 13.

Fig. 17. Side way image with non-flat ground and disparity image.

(a) (b)

Fig. 18. V-Disparity image and detected obstacles if ground is considered flat for image in Fig. 17.

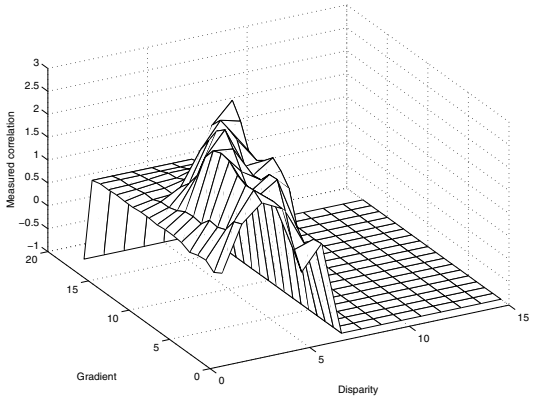

Fig. 19. Measured correlation plot for image in Fig. 17.

(a) (b)

Fig. 20. V-Disparity image and detected obstacles if ground is considered non-flat for image in Fig. 17.

VI. Conclusion

In a V-Disparity image the ground plane is simplified into a slanted line which is called ground correlation line in this paper. It could be straight if the ground is flat or curved if the ground is non-flat. The flat ground can be detected easily using Hough Transform, for non-flat ground, Labaynade [8] also used Hough Transform to extract two straight lines, but did not explain why the curved line can be decomposed into two straight lines. In this paper, we first analyzed the characteristic of ground correlation line of the non-flat ground plane with respect to the referee of the stereo vision system. Through the mathematical model of non-flat ground and the geometry of V-Disparity image, the ground correlation line can be considered as a combination of two straight line segments. We propose a method based on measured correlation accumulation along the candidate ground correlation lines, and choose the one having the highest accumulated value. Experimental results for on-road and off-road conditions show that the maximum of the accumulated value associated with candidate lines stands out, thus indicating the shape of the ground correlation line.

References

[1] A. Broggi, C. Caraffi, R. Fedriga, and P. Grisleri, "Obstacle detection with stereo vision for off-road vehicle navigation," *Computer Vision and Pattern Recognition, 2005 IEEE Computer Society Conference on*, vol. 3, no. 65- 65, pp. 20–26, June 2005.

[2] S. Se and M. Brady, "Ground plane estimation, error analysis and applications," *Robotics and Autonomous Systems*, vol. 39, no. 2, pp. 59 – 71, 2002.

[3] S. Badal, S. Ravela, B. Draper, and A. Hanson, "Practical obstacle detection and avoidance system," *IEEE Workshop on Applications of Computer Vision - Proceedings*, pp. 97 – 104, 1994.

[4] Q. Yu, H. Araujo, and H. Wang, "A stereovision method for obstacle detection and tracking in non-flat urban environments," *Autonomous Robots*, vol. 19, no. 2, pp. 141 – 157, 2005.

[5] P. Lombardi, M. Zanin, and S. Messelodi, "Unified stereovision for ground, road, and obstacle detection," *IEEE Intelligent Vehicles Symposium, Proceedings*, vol. 2005, pp. 783 – 788, 2005.

[6] X. Li, X. Yao, Y. L. Murphey, R. Karlsen, and G. Gerhart, "A real-time vehicle detection and tracking system in outdoor traffic scenes," *Proceedings - International Conference on Pattern Recognition*, vol. 2, pp. 761 – 764, 2004.

[7] G. Toulminet, M. Bertozzi, S. Mousset, A. Bensrhair, and A. Broggi, "Vehicle detection by means of stereo vision-based obstacles features extraction and monocular pattern analysis," *IEEE Transactions on Image Processing*, vol. 15, no. 8, pp. 2364 – 2375, 2006.

[8] R. Labayrade, D. Aubert, and J. Tarel, "Real time obstacle detection in stereovision on non flat road geometry through "v-disparity" representation," *Vehicle Symposium, 2002. IEEE*, vol. 2, pp. 646– 651, June 2002.

[9] J. Rebut, G. Toulminet, and A. Bensrhair, "Road obstacles detection using a self-adaptive stereo vision sensor: A contribution to the arcos french project," *IEEE Intelligent Vehicles Symposium, Proceedings*, pp. 738 – 743, 2004.

[10] J. Zhao, J. Katupitiya, and J. Ward, "Global correlation based ground plane estimation using v-disparity image," *Robotics and Automation, 2007 IEEE International Conference on*, pp. 529 – 534, 2007.

[11] R. Aufrere, R. Chapuis, and F. Chausse, "A model-driven approach for real-time road recognition," *Machine Vision and Applications, Springer-Verlag 2001*.

[12] S. Nedevschi, R. Danescu, D. Frentiu, T. Marita, F. Oniga, C. Pocol, T. Graf, and R. Schmidt, "High accuracy stereovision approach for obstacle detection on non-planar roads," *IEEE Inteligent Engineering Systems (INES)*, pp. 211 – 216, 2004.